Physik Daten
Physics Data

Optical Properties of Metals

Pt. II: Noble Metals, Aluminum, Scandium, Yttrium, the Lanthanides and the Actinides ($0.1 \lesssim h\nu \lesssim 500$ eV)

J. H. Weaver and C. Krafka
Synchrotron Radiation Center, University of Wisconsin Stoughton, Wisconsin 53589, USA

D. W. Lynch
Department of Physics, Iowa State University and Ames Laboratory USDOE
Ames, Iowa 50011, USA

E. E. Koch
Hamburger Synchrotronstrahlungslabor HASYLAB, DESY Hamburg, Germany

ISSN 0344–8401

1981

Nr. 18 – 2

Fachinformationszentrum Energie Physik Mathematik GmbH Karlsruhe

FACHINFORMATIONSZENTRUM ENERGIE · PHYSIK · MATHEMATIK GMBH KARLSRUHE

Physik Daten
Physics Data

Optical Properties of Metals

Pt. II: Noble Metals, Aluminum, Scandium, Yttrium, the Lanthanides and the Actinides ($0.1 \lesssim h\nu \lesssim 500$ eV)

		Sc	(Ti	V	Cr	Mn	Fe	Co	Ni)*	Cu	Al			
		Y	(Zr	Nb	Mo		Ru	Rh	Pd)*	Ag				
		La	(Hf	Ta	W	Re	Os	Ir	Pt)*	Au				
Ce	Pr	Nd		Sm	Eu	Gd	Tb	Dy	Ho	Er	Tm	Yb	Lu	
Th		U			Am									

J. H. Weaver and C. Krafka
Synchrotron Radiation Center, University of Wisconsin[+]
Stoughton, Wisconsin 53589, USA

D. W. Lynch
Department of Physics, Iowa State University and Ames Laboratory USDOE[+]
Ames, Iowa 50011, USA

E. E. Koch
Hamburger Synchrotronstrahlungslabor HASYLAB, DESY
Hamburg, Germany

* See Volume I

[+] Work supported in part by NSF DMR 782 1080 and DOE-OBES-W 7405-Eng-82

1981 Nr. 18-2 ISSN 0344–8401

ACKNOWLEDGEMENTS

The authors are grateful for the encouragement of colleagues and the excellent support of their home laboratories. The optical measurements shown herein associated with two of the authors (Weaver and Lynch) often reflect collaboration with C. G. Olson of the Ames Laboratory. In our own original optical studies, we profited from the fine support of the Ames Laboratory, USDOE, and the Synchrotron Radiation Center, University of Wisconsin-Madison. We are grateful to M. J. Arttus for her dedication in preparing this manuscript; to B. Kaufner and W. Knaut for their skillful drawings of the many figures; to K. Weaver for encouragement; to colleagues who provided the results of their optical studies, published and unpublished; and to D. J. Peterman for computer assistance.

PREFACE

The ever increasing number of publications makes more and more difficult for scientists and engineers to extract, evaluate und finally select the physical data relevant to their work from the original literature. At the most, they may be able to do so in their special field of interest, but in all other cases they will have to rely on data compilations. So far, there are many fields of physics for which such data compilations are not available or which fail to meet the requirements due to the fact that only one edition is published which soon becomes outdated, or the reason being that they are too specific and therefore not suitable for general use. The present series »Physik Daten/Physics Data« was created with the aim to relieve this shortcoming by regularly publishing data compilations for special topics. These compilations are constantly brought up to date.

Data from all fields of physics are included. These data may be of an experimental or theoretical nature. In some cases, bibliographies will also be published. If a large number of data is available on tape, a description and a few examples of these data will be given in the respective issue of the series. The tapes containing these data will be supplied upon request by the Fachinformationszentrum Energie, Physik, Mathematik. The data compilations will be published as individual booklets with a special pamphlet for each data collection. This form of publication has two advantages. To begin with, it will be handy for the user and, secondly, old issues can easily be replaced by new ones. Depending on the subject, the accompanying text will be in English, in German, or in both languages.

Suggestions for improvements in the selection of subjects, contents, and lay-out of future issues are welcome. Authors who are interested in the preparation of data collections are invited to contact the editors.

These data compilations are established and edited on the initiative and in cooperation with the Deutsche Physikalische Gesellschaft.

The Editors

INTRODUCTION

We have collected in this volume data on the optical properties of the elemental noble metals, aluminum, the lanthanides including Sc and Y, and the actinides. A companion volume (Vol. I) considered the optical properties of the elemental transition metals Ti-Ni, Zr-Pd, and Hf-Pt. In this way we have gathered together for easy reference the optical properties of most of the elemental metals as they are known today, 1980.

In this data compilation we present tables summarizing the work that has been done for each element (techniques, sample preparation, spectral range, etc.). Figures for each element display the most frequently used optical quantities, i.e. the normal incidence reflectance or reflectivity, the real and imaginary parts of the frequency-dependent dielectric function or the optical conductivity, and the absorption coefficient. Tables of these quantities and the loss function are also given for each element.

This data compilation covers the wavelength range 25 Å $\leq \lambda \leq$ 25 μm or the photon energy range ~0.05 $\leq h\nu \leq$ 500 eV [$h\nu$(eV) = 12398/λ (Å)]. Most of the published data fall between ~1 eV and ~6 eV, in the range where photomultiplier detectors and conventional laboratory sources are available. In the vacuum ultraviolet for ~6 $\leq h\nu \leq$ 30 eV, synchrotron radiation sources, rare gas continua, and discrete line sources have been used to measure the reflectance at near normal incidence for the noble metals and aluminum but for few of the other metals discussed here. For photon energies of

~30-200 eV the absorption coefficient has been measured with synchrotron radiation for most of the metals but rarely at higher energy. Unfortunately, we have found that there is not a complete set of data for most of the metals throughout the entire range. Data for wavelengths shorter than about 25 Å are quite sparse because of the difficulty of obtaining monochromatic radiation, particularly between 1 and 3 keV. Monochromator development programs now underway at many synchrotron radiation facilities around the world should improve the situation within the next few years.

The comparative tables and figures which describe the available data point out regions where reliable data are not available or where the present data are still insufficient or ambiguous. In many cases when we seek to provide a set of "most reliable" optical data, we have chosen to use our own data, accumulated for many of these metals over the last ten years. The reader can readily compare those tabular results to the rest of the literature through perusal of the figures. For the heavy lanthanide metals and Sc and Y, we tabulate our data for both polarizations of the electric field vector $\vec{E}$ relative to the crystallographic ĉ-axis of the hcp lattice. For the lighter lanthanides we include no tabular results. Before using our tables, the reader should consult the Methods of Measurements and Errors section and that devoted to The Use and Misuse.

The data have been obtained from a number of sources. To supplement the references collected by the authors over the years, we have searched via computer the abstracts appearing in the Physics Abstracts and Chemistry Abstracts, the former from 1969 to present and the latter from 1970 to present. In addition we have solicited unpublished data from colleagues. We have omitted much of the data obtained in the 1950's and essentially

all data obtained before 1950. We have generally excluded nonspectral optical data, e.g. values of the complex refractive index obtained ellipsometrically at the wavelengths of one or several spectral lines, and emissivity measurements at one wavelength. It is inevitable that we have overlooked some data or reference that we would like to have included. For such omissions we apologize.

The compilation has a large number of applications. For example, reliable optical constants are needed to design multiple-layer films for application in solar-energy-systems or reflecting opitcal elements. The data can be used to obtain spectral emissivities for measurements of the temperatures of hot transition metals. Of course, it can be used for a fundamental comparison between experimental optical properties and those calculated from first principles.

We begin with several definitions, then briefly discuss methods of measurement and the associated errors of each. Finally, before presenting the data in tabular and pictorial form, we offer several caveats about the use of the data.

DEFINITIONS

In a macroscopic view, the propagation of electromagnetic waves in an absorbing medium is governed by a frequency-dependent conductivity, $\sigma(\omega)$, and a frequency-dependent dielectric constant, $\varepsilon(\omega)$[1-6]. These usually are combined into a frequency-dependent complex dielectric function $\tilde{\varepsilon} = \varepsilon_1 + i\varepsilon_2$, or a frequency-dependent complex conductivity, $\tilde{\sigma} = \sigma_1 + i\sigma_2$, with

$$\tilde{\varepsilon}(\omega) = 1 + 4\pi i\tilde{\sigma}(\omega)/\omega \qquad (1)$$

and $\varepsilon_1 = \varepsilon$ and $\sigma_1 = \sigma$. Note that a metal, with its finite conductivity at $\omega = 0$, has $\varepsilon_2(\omega) \to \infty$ as $\omega \to 0$, but this causes no problems in the wave equation.*

For non-cubic materials, $\tilde{\sigma}$ and $\tilde{\varepsilon}$ will be tensors[7,8], but for all elemental metals which have been measured this tensor is diagonal in the crystallographic axis system, and there are no more than three independent components. One should be aware, however, that evaporated films of non-cubic metals may not always have isotropic optical properties, for there often is a preferred texture, with close-packed planes preferred. In the ensuing discussion we assume, for simplicity, an optically isotropic metal, either a cubic crystal or randomly-oriented grains in a polycrystalline film.

---

* The time-dependent Maxwell's equations are Fourier analyzed. In complex notation the time dependence of all fields is then either $\exp(i\omega t)$ or $\exp(-i\omega t)$. Either may be used and the resultant real parts of the fields, the measurables, are the same. The choice of sign does, however, affect the signs of the imaginary parts of the optical functions. We have used $\exp(-i\omega t)$ which leads to the positive sign on the imaginary parts of the complex quantities above. This choice is more consistent with the microscopic interpretation of optical properties based on quantum mechanics. The other choice of sign also is widely used, however.

Optical studies describe the response of matter to an applied electromagnetic field at optical frequencies (~10^{16} Hz). As discussed above, this is done through the frequency-dependent complex dielectric function, $\tilde{\varepsilon}(\omega) = \varepsilon_1 + i\varepsilon_2$ or, equivalently, the complex conductivity, $\tilde{\sigma}(\omega) = \sigma_1 + i\sigma_2$, which are used with Maxwell's equations, but which are descriptions of the material being studied. These are fundamental quantities, and can be calculated quantum mechanically from microscopic models of the solid. Either represents the elementary excitation spectrum, i.e., ε_2 (interband) or σ_1 (interband) provides a measure of interband absorption. ε_2 (interband) can be written as

$$\omega^2\varepsilon_2 = \frac{e^2\hbar^2}{3\pi m^2} \sum_{if} \int_0^\infty d^3k |\langle f|p|i\rangle|^2 \, \delta(E_f(\bar{k}) - E_i(\bar{k}) - \hbar\omega), \qquad (2)$$

where the electric dipole approximation has been used for the electron-photon interaction Hamiltonian, $|i\rangle$ and $|f\rangle$ are the initial (occupied) and final (empty) states, and $\bar{k}$, the electron wave vector, has been conserved through direct transitions.

A complete calculation of ε_2 from first principles is difficult, but can be simplified by assuming that matrix elements are independent of $\bar{k}$, i.e. are constant throughout the Brillouin zone. Then

$$\omega^2\varepsilon_2 \propto \sum_{if} \int_0^\infty d^3k \, \delta(E_f(\bar{k}) - E_i(\bar{k}) - \hbar\omega), \qquad (3)$$

which is termed the joint density of states (JDOS). The JDOS reflects the shape of the electronic energy bands, but obscures any information regarding transition probability variation.

Evaluations of equations (2) or (3) for the transition metals have shown that structures in the experimental ε_2 can arise from extended volumes of k-space, and the importance of critical points is diminished in transition

metals. Further, it has been shown that volumes of k space which are removed from high-symmetry lines can be the source of interband structures.

The dielectric function for the transition metals also includes contributions from intraband absorption. The free-carrier or intraband (or free-electron or Drude) absorption is described by

$$\tilde{\varepsilon}(\omega) = 1 - \frac{\omega_p^2}{\omega(\omega+i/\tau)} \qquad (4)$$

where ω_p is the free-electron plasma frequency and τ is the electronic relaxation time. The plasma frequency is defined by $\omega_p^2 = 4\pi Ne^2/m$, where N is the number of electrons of mass m per unit volume. For a free-electron gas with $\omega\tau >> 1$, the absorptivity reduces to $A = 2/\omega_p\tau$ which is small. In figure 1, the free electron dielectric function is shown qualitatively. At low energy, ε_2 is large and positive while ε_1 is large and negative. Both approach zero with increasing photon energy; ε_1 ultimately crosses zero at the plasma frequency and approaches unity at infinite frequency. In an experimental spectrum of the dielectric function for a real metal, the deviation from this simple behavior can be taken as an indication of interband absorption; see Fig. 1 for sketches of free carrier behavior.

For transition metals, where the d bands intersect the Fermi level, interband absorption begins at arbitrarily low energy, and it is impossible to separate the interband and intraband contributions completely. Nevertheless, it may be possible to fit the measured spectrum with a Drude-like spectrum over a limited energy range. The Drude parameters obtained in that way should not be taken too seriously. Nevertheless, they are often useful for separating approximately the low-energy interband and intraband contributions to $\tilde{\varepsilon}(\omega)$ facilitating comparison of theory with experiment.

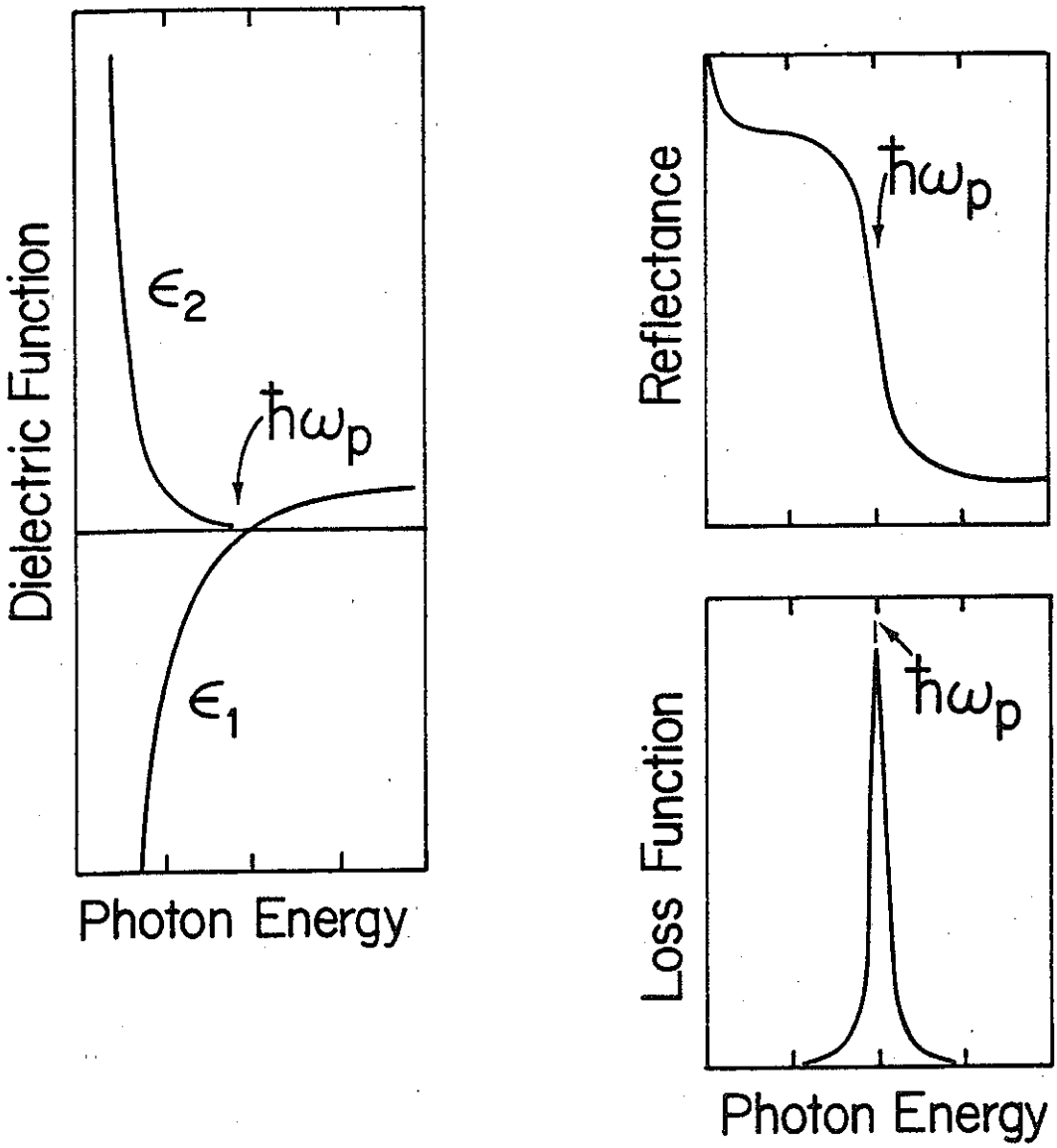

Fig. 1 Sketch of the reflectance of a free electron gas, its dielectric function, and its loss function.

The real and imaginary parts of the dielectric function are not completely independent. They are related in an integral-transform fashion by the so-called Kramers-Kronig or dispersion integrals:[2-5]

$$\varepsilon_1(\omega) - 1 = \pi^{-1} \; P \int_0^{\infty} \frac{\varepsilon_2(\omega') - \frac{4\omega\sigma(o)}{\omega'}}{\omega'^2 - \omega^2} \, \omega' d\omega' \tag{5}$$

$$\varepsilon_2(\omega) - \frac{4\pi\sigma(o)}{\omega} = \frac{-2\omega}{\pi} \; P \int_0^{\infty} \frac{\varepsilon_1(\omega') - 1}{\omega'^2 - \omega^2} \, d\omega' \tag{6}$$

where P denotes principal value. If a set of optical data such as $\varepsilon_1(\omega)$ and $\varepsilon_2(\omega)$ is self-consistent, it must satisfy the above relations, when suitable extrapolations to zero and infinity are appended to the data measured over some finite spectral range.

By letting $\omega \to \infty$, a limit in which we expect the electrons in the solid to behave as free electrons, we obtain the sum rule[2,5]

$$\int_0^{\infty} \omega\varepsilon_2(\omega) d\omega = 2\pi^2 \; \frac{Ne^2}{m} = \frac{\pi}{2} \omega_p^2 \tag{7}$$

which forms a very useful test of the data. This is equivalent to the f-sum rule of atomic physics. It states that the integral of ε_2 weighted by ω is proportional to N, the number density of electrons in the sample. By integrating to a finite upper limit, partial sum rules are obtained, but their use is somewhat restricted by assumptions necessary for their use.

There are several other sum rules[2,3] that are useful for testing data for consistency. These are

$$\int_0^{\infty} [\varepsilon_1(\omega) - 1] \, d\omega = -2\pi^2\sigma(o), \tag{8}$$

which relates the real part of the dielectric function to the d.c. conductivity, and

$$\int_0^\infty [n(\omega) - 1]d\omega = 0 \ , \tag{9}$$

which states that the average value of the refractive index is unity. These, and others[9-12], have been applied to optical data for aluminum and, to date, there are departures from self-consistency even when the best available data are used[13].

The boundary conditions on the electric and magnetic fields, implicit in Maxwell's equations[1-6], give values for the reflected and transmitted fields in terms of the dielectric function, $\tilde{\varepsilon}$, the angle of incidence, ϕ, and the state of polarization, s or p. If $\tilde{r}$ is the ratio of reflected electric field to incident electric field at a vacuum-solid interface, then[6]

$$\tilde{r} = \frac{\tilde{E}_r}{\tilde{E}_i} = (\tilde{g} - 1)/(\tilde{g} + 1) \tag{10}$$

with $\tilde{g} = \sqrt{\tilde{\varepsilon}} \cos \phi'$ for s-polarization

and $\tilde{g} = \cos \phi'/\sqrt{\tilde{\varepsilon}}$ for p-polarization,

in which $\sqrt{\tilde{\varepsilon}} \sin \phi' = \sin \phi$. The phase shift upon reflection, θ, is included in $\tilde{r}$ as $\tilde{r} = re^{i\theta}$. At this point it may be useful to introduce the complex index of refraction, defined* as

$$\tilde{N} = n + ik = \sqrt{\tilde{\varepsilon}} \ . \tag{11}$$

Then $\varepsilon_1 = n^2 - k^2$ and $2n^2 = (+\varepsilon_1 + \sqrt{\varepsilon_1^2 + \varepsilon_2^2})$

$\varepsilon_2 = 2nk$ $\quad 2k^2 = (-\varepsilon_1 + \sqrt{\varepsilon_1^2 + \varepsilon_2^2})$

---

* $\tilde{N}$ is sometimes written as $n(1 + iK)$.

If $\phi \to 0$ then the reflectance at normal incidence becomes

$$R = |\tilde{r}|^2 = \frac{(n-1)^2 + k^2}{(n+1)^2 + k^2} . \tag{12}$$

In any case, the measured reflectance is

$$R = |\tilde{r}|^2 . \tag{13}$$

The absorption coefficient μ is

$$\mu = 4\pi\, k/\lambda \tag{14}$$

where λ is the wavelength in vacuum and $\mu dx = -dI/I$ is the fractional loss of flux in distance dx, leading to the decay of the photon flux in the material as $\exp(-\mu x)$.

One can also study the optical properties of a solid with electrons rather than photons. The probability that a fast electron loses energy E in traversing a thin film of material with dielectric function $\tilde{\varepsilon}(E)$ is proportional to[14-16]

$$\mathrm{Im}(-1/\tilde{\varepsilon}) = \varepsilon_2/(\varepsilon_1^2 + \varepsilon_2^2) \tag{12}$$

By making suitable corrections to the measured intensity of the transmitted electron beam and by the use of a dispersion integral, it is possible to determine $\tilde{\varepsilon}(E)$. (There are additional corrections to be made for surface effects, for Čerenkov radiation, and for cases in which the incident electron is not sufficiently energetic.)

If the photon energy becomes high, larger than ~50 eV depending on the material, the above expressions simplify to

$$n = 1 - \delta \tag{13}$$

with $k \ll 1$ and $\delta \ll 1$. Then

$$\varepsilon_1 = n^2 - k^2 \approx 1, \tag{14}$$

$$R = \frac{(n-1)^2 + k^2}{(n+1)^2 + k^2} \approx \frac{\delta^2 + k^2}{4 - 2\delta} \ll 1 ,$$

$$\mathrm{Im}(-1/\tilde{\varepsilon}) \approx \varepsilon_2 .$$

A useful optical quantity in the visible and infrared is the spectral emissivity, $e(\omega)$, the fraction of blackbody radiation with a particular polarization emitted into a differential solid angle by the sample surface[17]. For an opaque sample with a flat surface this is equal to the absorptance, $A = 1 - R$, with the foregoing expressions giving R, the reflectance. (This is Kirchhoff's law.) The spectral hemispherical emittance is the sum of the integrals of the above emittance over 2π steradians for each polarization. The total hemispherical emittance at temperature T is the integral of the latter over the blackbody spectrum, divided by the blackbody spectral integral, both at temperature T. The hemispherical spectral emittance can be put into closed form as[18]

$$\sum_{pol} \frac{1}{\pi} \int_{hemis} e_{pol}(\omega,\alpha,\beta) \cos\alpha d\Omega = 4n - 4n^2 \ln\left(\frac{1 + 2n + n^2 + k^2}{n^2 + k^2}\right) \quad (18)$$

$$+ \frac{4n(n^2 - k^2)}{k} \tan^{-1}\left(\frac{k}{n + n^2 + k^2}\right)$$

$$+ \frac{4n}{n^2 + k^2} - \frac{4n^2}{(n^2 + k^2)^2} \ln(1 + 2n + n^2 + k^2)$$

$$+ \frac{4n(n^2 - k^2)}{k(n^2 + k^2)} \tan^{-1}\left(\frac{k}{1 + n}\right) .$$

where $d\Omega = \sin\alpha d\alpha d\beta$. α and β are the polar and azimuthal angles ($\alpha = \phi$, the angle of incidence used previously, and often there is no β-dependence). [The factor of π represents $\int_{hemis} 1 \cos\alpha d\Omega$, the spectral hemispherical emissivity of a blackbody of unit spectral emissivity, i.e. the normalizing factor.]

METHODS AND MEASUREMENT AND ERRORS

In general, any measured quantity can be expressed in terms of ε_1 and ε_2, or n and k, but, since both real and imaginary parts of the dielectric function appear in the expression, two measurements are needed at each frequency to obtain two equations from which $\tilde{\varepsilon}$ or $\tilde{N}$ can be found. There are four general categories of measurement: (1) photometric, (2) photometric with dispersion integrals, (3) ellipsometric, and (4) electron energy loss with dispersion integrals. Space limitations preclude a detailed discussion of each, but a few general statements seem to be in order[19].

(1) Photometric[20-40]. Two quantities involving the reflected photon flux, or possibly the flux transmitted through thin films, are measured. Examples are the reflectance of p-polarized light at two angles of incidence; the angle at which the p-polarized reflectance is a minimum and the value of R_p there; and even R_p and $dR_p/d\phi$ at some ϕ. More than two measurements may be made, e.g. R_p vs. ϕ, and the data fitted to $R_p(\phi)$. Experimental errors may involve all of the following: nonlinearity of the detector, nonhomogeneity and polarization sensitivity of the detector, failure to collect all reflected flux, and the use of different surface areas if two angles of incidence are used. These measurement errors may be very difficult to estimate. If an estimate can be made, it is relatively easy to determine how the errors will propagate to produce errors in n and k. Such an error analysis can be used to select the best, or at least better, quantities to measure for a sample of assumed optical properties. In general there is not a universal best method. The sample, its properties, and the wavelength region make some methods better than others.

(2) Photometric with dispersion integrals[2,5,41-55]. Here one measures R at fixed ϕ (often near-normal incidence) and fixed polarization over as wide a frequncy range as possible. The real and imaginary parts of the reflection coefficient $\tilde{r} = re^{i\theta}$ or of

$$\ln r = \ln(re^{i\theta}) = \ln(\sqrt{R}e^{i\theta}) = \tfrac{1}{2}\ln R + i\theta \qquad (19)$$

obey a dispersion or Kramers-Kronig integral. With suitable extrapolations beyond the range of the data, one can obtain $\theta(\omega)$ from $R(\omega)$. Errors in the measured reflectance then appear in the derived dielectric function as with other methods, but there are additional errors associated with the extrapolations. In general, the extrapolation errors affect the magnitude of ε_1 and ε_2 much more than they affect the positions and shapes of spectral structures. We have found, for example, that in Mo our dielectric function results obtained using dispersion integrals and measurements of $R(\omega)$ for 0.1-30 eV agree with $\tilde{\varepsilon}$ data obtained by photometric and ellipsometric methods to within 10%, while an error analysis yields an estimate of possible errors of up to 50%.

The availability of some transmission or electron energy loss data above 30 eV reduces the expected extrapolation errors, as does requiring the extrapolation to give reasonable values for the sum rule on ε_2 in the region of the extrapolation. A "variation" of the Kramers-Kronig method is to fit a reflectance spectrum with a series of oscillators, whose dielectric function then is represented by that of the sum of oscillators[56-57].

(3) Ellipsometric[58]. The ratio of reflected electric fields for p- and s-polarization is

$$\tilde{r}_p/\tilde{r}_s = (r_p/r_s)e^{i(\theta_p-\theta_s)} = \rho e^{i\Delta} \qquad (20)$$

The change in the state of polarization of reflected light can be measured,

giving ρ and Δ, from which $\tilde{\varepsilon}$ can be found. Ellipsometry has been carried out on metals since the time of Drude, but only relatively recently have data been taken at more than a few discrete wavelengths. Automatic ellipsometers now exist, often yielding $\tilde{\varepsilon}$ vs. ω directly with an on-line computer. Errors in ellipsometry can be different from those in photometry. The alignment of the polarizing elements is very important and can lead to errors. Ellipsometry is rarely carried out at energies above 6 eV for lack of effective polarizing elements.

(4) Electron energy loss[14-16]. As mentioned previously, energy analysis of energetic electrons passing through thin films can give $\mathrm{Im}(-1/\tilde{\varepsilon})$. This quantity is related to $\mathrm{Re}(-1/\tilde{\varepsilon})$ by a dispersion integral. Thus with suitable extrapolations, and possibly with a normalization factor based on other data, $\tilde{\varepsilon}$ can be obtained. In the measurement of electron energy loss spectra one must subtract out not only the surface losses but also multiple losses. In fact, the response of the solid to fast electrons is governed by the longitudinal dielectric function while the response to photons is governed by the transverse function. To date, experimental differences between them are negligible for purposes of this document.

All these methods are difficult to apply to metals in the infrared because $R \to 1$ for all ϕ and $\rho \to 1$. For photometric methods one can measure the absorptance, $A = 1 - R$, in methods (2) or use large angles of incidence in methods (1). In ellipsometry one can also use large angles of incidence and multiple (m) reflections to obtain $\rho^m \exp(im\Delta)$. Finally, electron energy loss measurements usually do not have sufficient resolution to be used for metals in the infrared, i.e. $h\nu \lesssim 1$ eV, since the zero-loss spectrum may have a width of up to 0.5 eV.

Above ~30 eV the reflectance of all materials quickly falls to values below 0.01 except at large angles of incidence. The primary methods of

determining $\tilde{\varepsilon}(\omega)$ then consist of fitting R vs. ϕ for large values of ϕ, transmission measurements which give μ, or electron energy loss measurements which then require significant corrections for multiple scattering. The latter two require the use of dispersion integrals to get real and imaginary parts of $\tilde{\varepsilon}$. New types of errors arise, such as pinholes in thin-film samples, increased scattering from surface roughness as the wavelength decreases, and incompletely collimated radiation.

In all cases the most important kinds of error have not yet been mentioned. All methods make use of the Fresnel relations, derived for a flat smooth interface between two media. (This is so for the electron energy loss measurements, too, for the surface corrections rely on a description of the interface between the sample and vacuum.) Surface roughness, oxide films, and surface stresses all cause errors because the actual sample departs from the ideal strain-free material with a smooth, abrupt vacuum interface. The errors which can arise from these departures from ideality are different for each type of measurement. A rough surface, for example, will make the measured reflectance too low if any scattered radiation fails to reach the detector[59-63]. A new structure, typically a reflectance dip, may appear in the reflectance if non-radiative surface plasmons are excited at the rough surface. Ellipsometric methods are less sensitive to roughness, but only insofar as the scattered radiation is not preferentially of one polarization. A transparent oxide will lower the measured reflectance, but in the infrared such an effect is negligibly small for a metal, while submonolayer coverages of transparent oxides can be measured ellipsometrically, causing significant error if unsuspected. In the ultraviolet, oxides are strongly absorbing and cause significant errors in all types of measurement, but those sampling the bulk more than the surface, e.g. electron energy loss measurements, are less sensitive to oxides.

In order to obtain the dielectric function of a metal a strain-free, clean, flat crystalline surface is needed. In principle, the surface should be cleaned in situ, with cleanliness verified by Auger spectroscopy, and checked for crystallinity, and perhaps strain, by LEED or high-energy electron diffraction (RHEED). This must be done in ultra high vacuum to insure subsequent surface cleanliness. Only then should the optical properties be measured. Unfortunately, such studies have not been performed for most metals in even limited spectral ranges. Moreover, in data taken just at one or at a few fixed wavelengths on truly clean surfaces, evaluations of surface roughness have not been made. Most surface cleaning techniques e.g., Ar^+ bombardment followed by an anneal, can lead to roughened surfaces. Certainly the older techniques of cleaning by Ar^+ glow-discharge sputtering creates rough surfaces. One may have to choose between a rough, atomically clean surface and a smooth "dirty" one with a few monolayers of oxide, although in some cases a compromise may be reached. A compromise often used has been to electropolish the samples. This leaves a smooth, strain-free surface, but one with an overlayer of oxide, often containing Cl as well if perchloric acid, $H_2C\ell O_3$, is used as the electrolyte[64]. Such treatment causes little error in the infrared reflectance, but above about 6 eV the 2p electrons of oxygen absorb and cause errors. Of course the amount of error varies from sample to sample because of the oxidation processes itself; the oxidation rate also varies for different crystalline faces of a single crystal.

Thin films may be evaporated onto flat substrates, but they are inherently strained, polycrystalline samples. Strain will broaden structure in the optical spectra and the polycrystalline character may introduce special effects due to grain boundaries or voids. Annealing of the film

during deposition (hot substrate) or afterward will reduce the strain but at the expense of surface roughness. Recently it was shown that many conflicting spectra obtained on thin films of Au could be reconciled by assuming different degrees of porosity in the films, up to 10% maximum. In general, such voids lower the magnitudes of ε_1 and ε_2, an effect which can be viewed in zero order as an averaging in the dielectric function of the film with that of the voids, approximated by vacuum[65]. The spectra of many films measured over the years have agreed in shape but not in magnitude. In another view of grain boundaries in films the infrared energy dependence of $\tilde{\varepsilon}(\omega)$ has been interpreted with a two-medium model in which the grain boundary material has a lower electron density and a higher electron scattering (damping) rate[66,67].

For purposes of calculating mirror or interference filter performance, it may be desirable to use data taken on films, voids and all, in order to model better the performance of samples which will, in fact, be vapor deposited films. For this purpose, the tabular data reported in this volume are less suitable than some of the data we have shown in our comparison figures since the tabular data were measured with bulk samples. Furthermore, for some of the hcp metals we present tabular data for oriented single crystals with $\vec{E} \parallel \hat{c}$ and $\vec{E} \perp \hat{c}$ to display the optical anisotropy of the material. In principle, for a polycrystalline film with randomly-oriented grains, $\tilde{\varepsilon}(\omega) = 1/3\ \tilde{\varepsilon}_{\parallel}(\omega) + 2/3\ \tilde{\varepsilon}_{\perp}(\omega)$, but in practice the film may grow preferentially with basal plane orientation along the surface ($\hat{c}$ perpendicular to the surface).

USE AND MISUSE OF THE DATA

The data presented in this document represent our assessment of the literature. Some idea of the discrepancies between the data presented and other data is also given. A glance at some of the data we do not present but list only by reference will show that there can be extremely large discrepancies, not only in the magnitudes of $\tilde{\varepsilon}$ and $\tilde{\sigma}$ but even in the occurrence and non-occurrence of spectral features. We believe that the data tabulated are good to within ±10% in most cases (except near places where ε_1 crosses zero, for which a relative error is meaningless). The potential user should keep this 10% figure in mind for critical applications. Exceptions can be identified by examination of the figures.

The data are intended to represent the optical properties of pure, flat, strain-free, oxide-free samples. Effects of overlayers can be calculated in a straightforward manner. Departures from flatness are another matter. Slight surface roughness can be handled but in extreme cases, such as gold black or dendritic tungsten surfaces, the optical properties of the sample do not resemble those of the metal at all, purely for morphological reasons. The data could, however, be used to model such materials and cermets unless the particle size becomes too small.

We should also mention that the data are appropriate only for the normal room temperature or liquid helium temperature phase of the material. The data for fcc Ni are not at all close to those for amorphous Ni (not given), nor can the data for bcc Fe be used for the high temperature fcc phase of that metal. The effects of magnetic ordering are less extreme, but are sometimes important. For example, the data for Cr taken at 4.2 K show a small peak near 0.1 eV which is a result of the antiferromagnetic

ordering. As the temperature increases, this peak weakens and broadens and is very difficult to see at room temperature, even though Cr is still antiferromagnetic.

The functions $\tilde{\varepsilon}$ and $\tilde{\sigma}$ can be calculated theoretically. As presented here they are local functions, i.e. the material is presumed to have no special effects due to the surface, and the anomalous skin effect has been ignored in obtaining $\tilde{\varepsilon}$ from the measured data. This latter effect[2,5] can be significant for single crystals at and below room temperature in the near, and especially the far, infrared. The data can be applied without correction to evaporated films, whose mean free path is usually short. To deal properly with single crystals in the infrared, whenever interband absorption does not dominate, one should abandon the $\tilde{\varepsilon}$ concept and work with the reflectance itself or the surface impedance[2], $\tilde{Z} = (4\pi/c)\tilde{E}/\tilde{H}$, where the fields are the tangential components evaluated at the surface. Then $\tilde{r} = (4\pi/c-\tilde{Z})/(4\pi/c+\tilde{Z})$ at normal incidence.

Finally, we have presented room temperature or liquid helium temperature data only. Many applications require data at high temperature, e.g., optical pyrometry and solar-thermal energy applications. Provided oxides or surface roughness do not increase at the higher temperatures, one can use the room temperature data for many applications. There are two ways to obtain the temperature dependence. One can make measurements, e.g. of the reflectance at all temperatures of interest, but in addition to the problems of enhanced oxidation and possible surface roughening at high temperature, problems with sample evaporation and the blackbody radiation of the sample itself arise. At temperatures above ~1000 K the emissivity is usually what is measured, by comparing the radiation from the sample with that from a cavity, often in the sample itself. The other method

measures directly the temperature derivative of the reflectance or absorptance of the sample, by modulation spectroscopic techniques with a calibration determined by a steady-state calorimetric method.

REFERENCES

1. M. Born and E. Wolf, "Principles of Optics". (Pergamon Press, London, 1959).

2. F. Stern, Solid State Physics 15, 299 (1963).

3. L.D. Landau and E.M. Lifshitz, "Electrodynamics of Continuous Media", (Addison-Wesley, Reading, Mass., 1965).

4. A.V. Sokolov, "Optical Properties of Metals", (Blackie, London, 1967).

5. F. Wooten, "Optical Properties of Solids", (Academic, New York, 1972).

6. H. Wolter, Handbuch der Physik 24, 461 (1956).

7. J.F. Nye, "Physical Properties of Crystals", (Oxford University Press, London, 1957).

8. C.S. Smith, Solid State Physics 6, 175 (1958).

9. M. Altarelli, D.L. Dexter, H.M. Nussenzveig, and D.Y. Smith, Phys. Rev. B 6, 175 (1958).

10. A. Villani and A.H. Zimmerman, Phys. Rev. B 8, 3914 (1973).

11. M. Altarelli and D.Y. Smith, Phys. Rev. B 9, 1290 (1974); B 12, 3511 (1975).

12. D.Y. Smith, Phys. Rev. B 12, 5303 (1976).

13. E. Shiles, T. Sasaki, M. Inokuti, and D.Y. Smith, Phys. Rev. B 22, 1612 (1980).

14. H. Raether, "Springer Tracts in Modern Physics", Vol. 38 (Springer-Verlag, Berlin, 1965).

15. J. Daniels, C.v. Festenberg, H. Raether, and K. Zeppenfield, "Springer Tracts in Modern Physics", Vol. 54 (Springer-Verlag, Berlin, 1970).

16. H. Raether, "Springer Tracts in Modern Physics", Vol. 88 (Springer-Verlag, Berlin, 1980).

17. H.P. Baltes, "Progress in Optics", XIII, 1 (1976) ed. E. Wolf.

18. R. Siegel and J.R. Howell, "Thermal Radiation Heat Transfer", (McGraw-Hill, New York 1972) p. 109.

19. D.W. Lynch, J. de Physique Suppl. 77, 15-21 (1977).

20. I. Simon, J. Opt. Soc. Am. 41, 334 (1951).

REFERENCES (cont'd)

21. W.R. Hunter, J. Opt. Soc. Am. 55, 1197 (1965).

22. W.R. Hunter, Appl. Opt. 6, 2140 (1967).

23. D.G. Avery, Proc. Phys. Soc. (London) B65, 425 (1952).

24. R.E. Lindquist and A.W. Ewald, J. Opt. Soc. Am. 53, 247 (1963).

25. B.F. Armally et al., Appl. Opt. 11, 2907 (1972).

26. S.P.F. Humphreys-Owen, Proc. Phys. Soc. (London) 77, 949 (1961).

27. R.F. Potter, J. Opt. Soc. Am. 54, 904 (1964).

28. R.F. Potter, Appl. Opt. 4, 53 (1965).

29. O. Hunderi, Appl. Opt. 11 1572 (1972).

30. A. Balzarotti, P. Picozzi, and S. Santucci, Surf. Sci. 37, 994 (1973).

31. W.R. Hunter, J. Opt. Soc. Am. 54, 15 (1964); 55, 1197 (1965).

32. U.S. Whang, E.T. Arakawa, and T.A. Callcott, J. Opt. Soc. Am. 61, 740 (1971).

33. U.S. Whang, E.T. Arakawa, and T.A. Callcott, Phys. Rev. B 5, 2118 (1972); B 6, 2409 (1972).

34. P.O. Nilsson, Appl. Opt. 7, 435 (1968).

35. F. Abeles and M.L. Theye, Surf. Sci. 5, 325 (1966).

36. G. Baldini and L. Rigaldi, J. Opt. Soc. Am. 60, 495 (1970).

37. L. Ward and A. Nag, Brit. J. Appl. Phys. 18, 277 (1967).

38. L. Ward and A. Nag. J. Phys. D 3, 462 (1970).

39. R.F. Miller, A.J. Taylor, and L.S. Julien, J. Phys. D 3, 1957 (1970).

40. J.E. Nestell and R.W. Christy, Appl. Opt. 11, 643 (1972).

41. R.A. MacRae, E.T. Arakawa, and M.W. Williams, Phys. Rev. 162, 615 (1967).

42. B.W. Veal and A.P. Paulikas, Phys. Rev. B 10, 1280 (1974).

43. D.E. Thomas, Bell Syst. Tech. 26, 870 (1947).

44. E.L. Krieger, D.J. Olechna, and D.S. Story, General Electric Corp. Report No. 63-RL-3458G, September 1963.

REFERENCES (cont'd)

45. P.O. Nilsson and L. Munkby, Phys. Kond. Mat. 10 290 (1969).

46. B. Velicky, Czech. J. Phys. B 11, 787 (1961).

47. V.K. Miloslavskii, Opt. Spectroscop. 21, 193 (1961).

48. D.M. Roessler, Brit. J. Appl. Phys. 16, 1359 (1965).

49. G. Leveque, J. Phys. C 10, 4877 (1977).

50. D.W. Berreman, Appl. Opt. 6, 1519 (1967).

51. G.M. Hale, W.E. Holland, and M.R. Querry, Appl. Opt. 12, 48 (1973).

52. C.W. Peterson and B.W. Knight, J. Opt. Soc. Am. 63, 1238 (1973).

53. D.M. Roessler, Brit. J. Appl. Phys. 17, 1313 (1966).

54. R. Klucker and U. Nielsen, Computer Phys. Comm. 6, 187 (1973).

55. D.Y. Smith, J. Opt. Soc. Am. 67, 570 (1977).

56. H.W. Verleur, J. Opt. Soc. Am. 58, 1356 (1968).

57. J. Rivory, Optics Commun. 1, 334 (1970).

58. D.E. Aspnes, "Optical Properties of Solids, New Developments", (North Holland, Amsterdam, 1976) ed. B.O. Seraphin, p. 799.

59. H.E. Bennett and J.M. Bennett, "Physics of Thin Films", Vol. 4 (Academic Press, New York, 1967) ed. G. Hass and R.E. Thun, p. 1.

60. H.E. Bennett and J.O. Porteus, J. Opt. Soc. Am. 51, 123 (1961).

61. H.E. Bennett, J. Opt. Soc. Am. 53, 1389 (1963).

62. J.O. Porteus, J. Opt. Soc. Am. 53, 1294 (1963).

63. D.W. Berreman, Phys. Rev. 163, 855 (1967); B 2, 381 (1970).

64. A.J. Bevolo, B.J. Beaudry, and K.A. Gschneidner, Jr., J. Electrochem. Soc. 127, 2556 (1980).

65. D.E. Aspnes, Phys. Rev. B 21, 3290 (1980).

66. O. Hunderi, Phys. Rev. B 15, 3419 (1973).

67. S.R. Nagel and S.E. Schnatterly, Phys. Rev. B 9, 1299 (1974).

Table I. List of abbreviations used in the figures and tables.

$\varepsilon_1, \varepsilon_2$	real and imaginary parts of the complex dielectric function, $\tilde{\varepsilon}(\omega) = \varepsilon_1 + i\varepsilon_2$
$-\mathrm{Im}(\tilde{\varepsilon}^{-1}), -\mathrm{Im}(\tilde{\varepsilon}+1)^{-1}$	volume and surface loss functions
KK	Kramers-Kronig analysis
μ	absorption coefficient
RT	room temperature, ~300 K
n,k	index of refraction and extinction coefficient, $\tilde{N}(\omega) = n + ik$
σ	optical conductivity, $\sigma = \varepsilon_2\omega/4\pi$
T	temperature; transmission (if it appears in data presentation column)
A	absorptivity, A = 1 - R
R	reflectivity or reflectance
$\vec{E} \parallel \vec{c}$, $\vec{E} \perp \hat{c}$	$\vec{E}$ = electric field vector; $\hat{c}$ = crystallographic c-axis for hcp metals where c is orthogonal to the basal plane
$\varepsilon, \varepsilon_H, \varepsilon_N$	emissivity, hemispherical emissivity, normal emissivity
MP	mechanical polishing
Ex, In	ex situ, in situ
uhv	ultra high vacuum (generally ~10^{-9} Torr or better)
TEM	transmission electron microscopy
LEED	low energy electron diffraction
AES	Auger electron spectroscopy
Trans	transmission
Refl	reflection
m-θ	multi-angle
Ellips	ellipsometry
Sput	Argon-sputtering, generally implies post-sputtering annealing
EP	electropolish
CP	chemically polished